Biology of Reproduction, 2019, 100(4), 1066–1072
doi:10.1093/biolre/ioy245
Research Article
Advance Access Publication Date: 18 November 2018

Research Article

Loss-of-function mutations with circadian rhythm regulator Per1/Per2 lead to premature ovarian insufficiency†

Yating Zheng [1], Chao Liu[1], Yan Li[1], Haijuan Jiang[1], Peixin Yang[2], Jing Tang[3], Ying Xu [4], Han Wang [5] and Yulong He [1,*]

[1]Cyrus Tang Hematology Center, Collaborative Innovation Center of Hematology, State Key Laboratory of Radiation Medicine and Protection, Jiangsu Key Laboratory of Preventive and Translational Medicine for Geriatric Diseases, Soochow University, Suzhou, China; [2]Department of Obstetrics, Gynecology and Reproductive Sciences, University of Maryland School of Medicine, Baltimore, USA; [3]Institute for Molecular Medicine Finland (FIMM), University of Helsinki, Helsinki, Finland; [4]Cam-Su Genomic Resources Center, Soochow University, Suzhou, China and [5]Center for Circadian Clocks, Soochow University, Suzhou, China

*__Correspondence:__ Cyrus Tang Hematology Center, Collaborative Innovation Center of Hematology, State Key Laboratory of Radiation Medicine and Protection, Jiangsu Key Laboratory of Preventive and Translational Medicine for Geriatric Diseases, Soochow University, 199 Ren-Ai Road, Suzhou, China. Tel: +86-512-65880877; Fax: +86-512-65880929; E-mail: heyulong@suda.edu.cn

†__Grant Support:__This work was supported by grants from the Ministry of Science and Technology of China (2012CB947600), the National Natural Science Foundation of China (91539101, 81770489, 91739304), and the Priority Academic Program Development of Jiangsu Higher Education Institutions.
YZ, CL and YL contributed equally to this work.

Received 15 March 2018; Revised 31 August 2018; Accepted 16 November 2018

Abstract

The mechanism underlying premature ovarian insufficiency remains incompletely understood. Here we report that mice with *Per1*$^{m/m}$*; Per2*$^{m/m}$ double mutations display a decrease in female fertility starting approximately at 20 weeks old, with significantly less pups born from 32 weeks old onwards. Histological analysis revealed that a significant reduction of ovarian follicles was observed in the *Per1/Per2* mutants compared with the littermate controls examined at 26 and 52 weeks old, while the difference was not statistically significant between the two groups at 3 and 8 weeks old. We further showed that vascular development including the ovarian follicle associated vascular growth appeared normal in the *Per1/Per2* mutant mice, although clock genes were reported to regulate angiogenesis in zebrafish. The findings imply that loss-of-function mutations with Per1/Per2 result in a premature depletion of ovarian follicle reserve leading to the decline of reproductive capacity.

Summary Sentence

Disruption of circadian rhythm or its underlying regulatory network contributes to the premature depletion of ovarian follicle reserve.

Key words: PER1, PER2, ovarian follicle, ovarian insufficiency, knockout mouse.

Introduction

Premature ovarian insufficiency (POI) is characterized by a loss of ovarian function in women at reproductive ages, and is a heterogeneous condition with genetic, environmental, and other causes such as iatrogenic factors [1, 2]. The cyclic process of ovarian follicular development includes the follicle growth and maturation, ovulation,

as well as corpus luteum formation. The ovarian events are tightly controlled by the circadian system, as shown by the rhythmic hormone release in the hypothalamus–pituitary–ovary axis [3].

Circadian rhythms exist in diverse life forms and modulate the transcriptional activity of numerous genes in both suprachiasmatic nuclei (SCN) and peripheral tissues including the reproductive system [4–6]. The molecular machinery of the circadian clock is a feedback loop of core regulators including the transcriptional activators BMAL1 and CLOCK, as well as the repressors PER1–3 and CRY1–2 in mammals [4–6]. PER1 and PER2 are critical in the regulation of circadian rhythmicity, and mice deficient in *Per1* or *Per2* displayed a short circadian period [7, 8]. Double mutations of *Per1/Per2* genes disrupted circadian rhythms in locomotor activity and the expression of key clock genes as well as clock-regulated genes [7–9]. Both *Per1* and *Per2* mRNA were found to have a rhythmic oscillation in rat ovaries [10, 11], and were expressed in pituitary and hypothalamus that may participate in the coordination of GnRH (gonadotropin-releasing hormone) and LH (luteinizing hormone) surge [3, 7, 12–14]. Consistently, loss-of-function mutations with mouse *Per1* or *Per2* were reported to have a lower reproductive success in female mutants after 9 months old [15]. Irregular estrous cycles and lack of a coordinated LH surge were also observed in *Clock* mutants [16]. Knockout of *Bmal1* led to impaired fertility due to the disruption of steroidgenesis and implantation [17–19], and Bmal1 deficiency in ovarian thecal cells was found to disrupt ovulation due to the alteration of the phasic sensitivity to LH [20].

In the circulatory system, PER2 mutation was shown to impair vascular endothelial function [21], and PER2 and BMAL1 were reported to have a role in the regulation of developmental angiogenesis in zebrafish [22]. The ovarian follicular development is accompanied by active angiogenesis [23]. To investigate the mechanism underlying the reproductive defects of *Per1* and *Per2* mutants, we analyzed the vascular growth in ovaries and other tissues of *Per1/Per2* doubly mutant mice in this study. We found that loss-of-function mutations with *Per1/Per2* genes led to the reduced female fertility resulting from the premature decrease of ovarian follicles, but did not produce any obvious effect on vascular growth during the follicular development.

Materials and methods

Animal models

Mice with mutations targeting *Per1* and *Per2* genes were generated, as previously described [7, 8]. We obtained the breeding pairs of *Per1* and *Per2* single mutants, and the doubly mutant mice ($Per1^{m/m}$; $Per2^{m/m}$) were generated by two rounds of mating. The genetic background of *Per1/Per2* doubly mutant and control mice are C57/BL6. All animal experiments were performed in accordance with the institutional guidelines of the Soochow University Animal Center. In all the phenotype analysis, littermates were used as control.

Quantification of litter and pup number

To assess reproductive performance, the doubly mutant ($Per1^{m/m}$; $Per2^{m/m}$, 8 weeks old) and littermate control female mice ($Per1^{+/m}$; $Per2^{+/m}$) were mated with age-matched male mice (B6 background). The total number of litters and pups for each female mouse were recorded up to 52 weeks old.

Histological analysis of ovarian follicles

Ovaries of $Per1^{m/m}$; $Per2^{m/m}$ mutant and littermate control female mice (3, 8, 26, or 52 weeks old) were fixed in 4% PFA (paraformaldehyde) and embedded in paraffin. Serial sections (8 μm) were collected and stained with hematoxylin-eosin. The number of follicles with oocyte nuclei in every fifth section was counted and used for calculating the total number of follicles per ovary. The criteria for classifying developmental stages of ovarian follicles were as follows: primordial follicle, oocyte surrounded by a single layer of flattened follicular epithelial cells; primary follicle, oocyte surrounded by a single layer of cuboidal follicular cells; secondary follicle, oocyte surrounded by multiple layers of follicular cells; antral follicle: oocyte surrounded by granulosa cells containing also a fluid filled cavity.

Immunostaining

For whole-mount immunostaining with skin and retina, tissues were harvested and processed as previously described [24]. The antibodies used were rat anti-mouse PECAM-1 (platelet endothelial cell adhesion molecule 1; BD Pharmigen, 553370), rabbit anti-mouse LYVE-1 (lymphatic vessel endothelial hyaluronan receptor; Abcam, ab14917), and rabbit-anti-mouse cleaved Caspase-3 (Cell Signaling Technology, 9661S). Alexa488- and Alexa594 (Invitrogen)-conjugated secondary antibodies were used for staining. Slides were mounted with Vectashield (VectorLabs) and analyzed with the Olympus FluoView 1000 confocal microscope. For staining of frozen sections, ovary and uterus tissues were collected and processed as previously described [24]. Consecutive sections (10 μm in thickness) were incubated with antibodies against PECAM-1 and LYVE-1, followed by staining with the appropriate fluorochrome-conjugated secondary antibodies and mounted as described above. For the quantification of blood vessel parameters in the retina, fluorescent images were taken from similar regions in all samples and analyzed by using Image Pro Plus (Media Cybernetics).

Statistical analysis

Statistical analysis was performed with the unpaired *t* test. All statistical tests were two-sided. Data are presented as mean ± SD.

Results

Early onset of fertility decline with *Per1/Per2* doubly mutant female mice

Per1/Per2 doubly mutant mice were shown to be arrhythmic [7, 25]. To investigate the effect and underlying mechanism of *Per1/Per2* mutations on female reproduction, we set up mating using $Per1^{m/m}$; $Per2^{m/m}$ doubly mutant female mice starting from 8 weeks old, and the heterozygous $Per1^{+/m}$; $Per2^{+/m}$ littermate mice were used as control. Quantification of accumulated litter and pup number from the mutant and control mice is shown in Figure 1A and B, and Table 1. A trend of decrease of litter and pup number was already obvious starting from 20 weeks old, and a statistically significant difference in female fertility was observed from 32 weeks old onwards between the mutant and control mice. However, there was no significant difference in litter size (pups per litter recorded from 8 to 52 weeks old, $Per1^{m/m}$; $Per2^{m/m}$: 6.56 ± 0.99, n = 12; $Per1^{+/m}$; $Per2^{+/m}$: 6.85 ± 1.41, n = 11; $P = 0.5714$). It is also worth noting that few pups were born from $Per1^{m/m}$; $Per2^{m/m}$ mutants after 44 weeks old (Table 1).

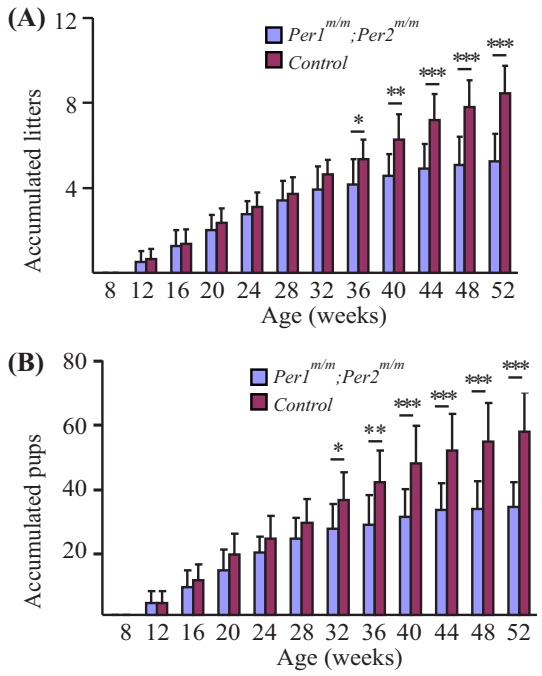

Figure 1. Quantification of accumulated litter and pup number of *Per1*$^{m/m}$*; Per2*$^{m/m}$ doubly mutant and control mice. (A) Quantification of litter number of *Per1*$^{m/m}$*; Per2* $^{m/m}$ mutant and control mice. (B) Pup number of *Per1*$^{m/m}$*; Per2*$^{m/m}$ mutant and control mice.

Premature ovarian follicle insufficiency in *Per1/Per2* mutants

Although a number of genes and nongenetic factors have been identified contributing to the occurrence of POI, the involvement of circadian clock and its regulators in this pathogenesis is unclear. To analyze the effect of double *Per1/Per2* mutations on ovarian follicle development, ovaries from different ages of mice (3, 8, 26, and 52 weeks old) were collected for histological analysis of follicle number at primordial, primary, secondary, and antral stages (Figure 2A). Quantification of follicle number revealed that *Per1*$^{m/m}$*; Per2*$^{m/m}$ doubly mutant mice had similar number of primordial, primary, secondary, or antral ovarian follicles at the stages of 3 weeks old (Figure 2B) in comparison with those of control littermates. There was also no significant difference in the total number of ovairan follicles observed in the *Per1/Per2* mutant ovaries of 8-week-old mice (Figure 2C). However, a significant decrease in the number of ovarian follicles was detected at ages of 26 weeks old (Figure 2D) and 52 weeks old (Figure 2E) between the two groups (Table 2). Analysis by immunostaining with cleaved caspase-3 showed that there was no statistically significant difference in apoptotic cell number between the *Per1*$^{m/m}$*; Per2*$^{m/m}$ doubly mutant and control mice (Supplemental Figure S1; *Per1*$^{m/m}$*; Per2*$^{m/m}$: 53.35 ± 2.03, n = 3; *Control*: 51.69 ± 2.68, n = 3; $P = 0.4406$).

Angiogenesis in ovaries of *Per1/Per2* doubly mutant mice

It has been shown that morpholino-mediated knockdown of *per2* or *bmal1* altered the developmental angiogenesis in zebrafish [22]. To find out whether *Per1/Per2* mutations would affect vascular devel-

Table 1. Litter size and pup number of *Per1*$^{m/m}$*; Per2*$^{m/m}$ doubly mutant and control mice.

Age (weeks)	Number of accumulated litters		n (*Per1*$^{m/m}$;*Per2*$^{m/m}$)	n (*Control*)	*P* value
	Per1$^{m/m}$;*Per2*$^{m/m}$	*Control*			
Number of accumulated litters					
8	0	0	12	11	
12	0.50 ± 0.52	0.64 ± 0.50	12	11	0.53182939
16	1.25 ± 0.75	1.36 ± 0.67	12	11	0.70798791
20	2.00 ± 0.74	2.36 ± 0.67	12	11	0.23254607
24	2.75 ± 0.62	3.09 ± 0.70	12	11	0.22987128
28	3.42 ± 0.90	3.73 ± 0.79	12	11	0.39011313
32	3.92 ± 1.08	4.64 ± 0.67	12	11	0.07253613
36	4.17 ± 1.19	5.36 ± 0.92	12	11	0.01431332
40	4.58 ± 1.00	6.27 ± 1.19	12	11	0.00132172
44	4.92 ± 1.16	7.18 ± 1.25	12	11	0.00019715
48	5.08 ± 1.31	7.82 ± 1.25	12	11	4.6502E-05
52	5.25 ± 1.29	8.45 ± 1.29	12	11	6.6428E-06
Number of accumulated pups					
8	0	0	12	11	
12	3.58 ± 3.78	3.82 ± 3.79	12	11	0.88319599
16	8.58 ± 5.55	10.82 ± 5.13	12	11	0.32893069
20	14.08 ± 6.42	19.00 ± 6.45	12	11	0.0813109
24	19.75 ± 4.99	24.09 ± 7.12	12	11	0.10293094
28	24.08 ± 6.56	28.91 ± 7.42	12	11	0.11264827
32	27.17 ± 7.71	36.18 ± 8.75	12	11	0.01575296
36	28.42 ± 9.22	41.73 ± 10.04	12	11	0.00329245
40	30.83 ± 8.62	47.55 ± 11.80	12	11	0.00082026
44	33.00 ± 8.44	51.64 ± 11.58	12	11	0.00022759
48	33.42 ± 8.50	54.45 ± 12.13	12	11	8.5033E-05
52	33.92 ± 7.86	57.55 ± 12.23	12	11	1.604E-05

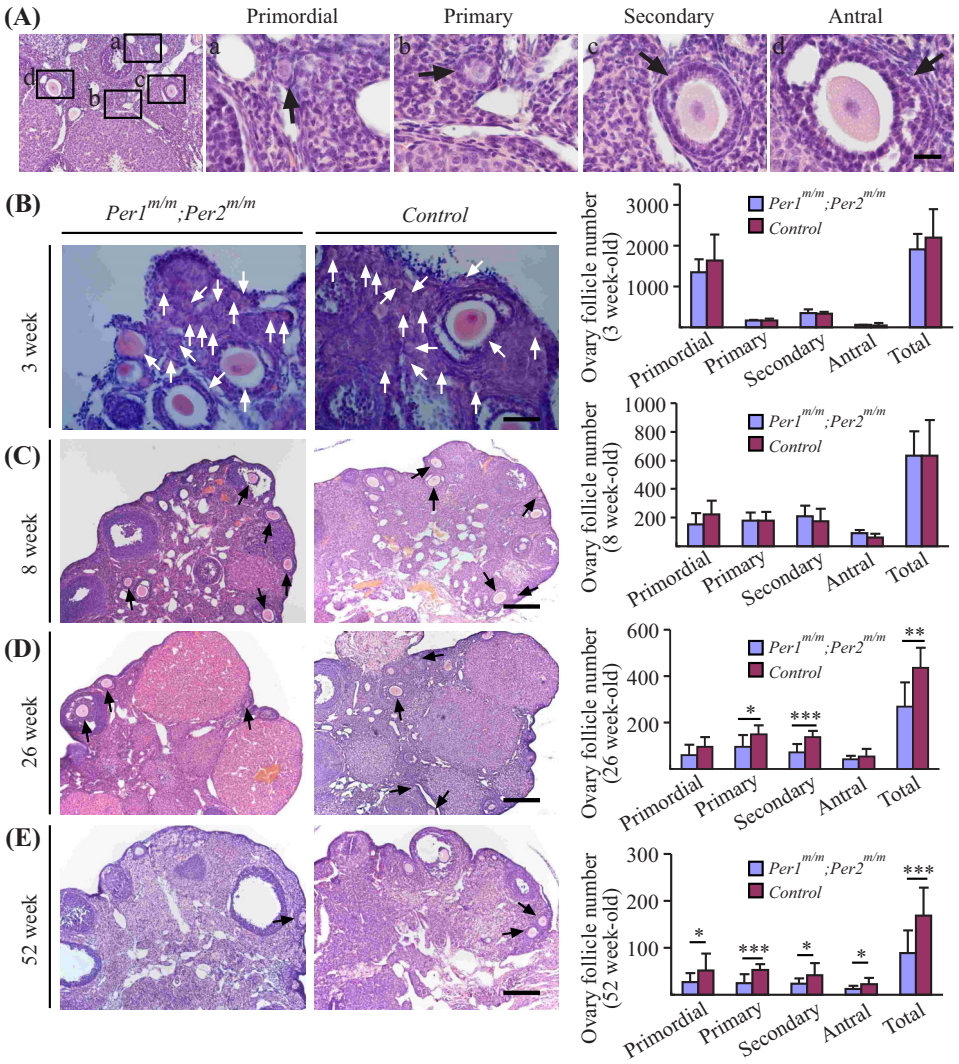

Figure 2. Analysis of ovarian follicle development in *Per1*$^{m/m}$*; Per2*$^{m/m}$ mutant and control mice. (A) Ovarian follicular development in wild-type mice at different stages including primordial, primary, secondary, and antral stages. (B–E) Histological analysis and quantification of ovarian follicle number at different ages, including 3, 8, 26, and 52 weeks old. Arrows indicate the follicles with oocyte nuclei for quantification. Scale bar: 20 μm in A, 50 μm in B, 200 μm in C–E.

opment including the cyclic angiogenesis during ovarian follicular development, we performed the fluorescence immunostaining with ovaries and several other tissues of *Per1*$^{m/m}$*; Per2*$^{m/m}$ mutant and control mice at different development stages. Quantification of retina vascularization area (P5, postnatal day 5) showed that there was no significant difference between *Per1*$^{m/m}$*; Per2*$^{m/m}$ mutant and wild-type ($P = 0.3644$) or the heterozygous control mice ($P = 0.5886$; WT: $46.25 \pm 2.93\%$, n = 6; *Per1*$^{+/m}$; *Per2*$^{+/m}$: $46.97 \pm 5.16\%$, n = 6; *Per1*$^{m/m}$*; Per2*$^{m/m}$: 48.52 ± 5.39, n = 9; Supplemental Figure S2A). Constistently, there was no difference detected in blood vascular and lymphatic vessels of skin (P5) between *Per1/Per2* mutant and controls (Supplemental Figure S2B). At the adult stage, blood vascular and lymphatic vessels also appeared normal in the ear skin, trachea, and uterus of *Per1*$^{m/m}$*; Per2*$^{m/m}$ mutant mice compared with those of the control (Supplemental Figure S3A–C). Consistently, there was no obvious difference in both blood vascular and lymphatic vessel growth associated with the ovarian follicles between *Per1/Per2* mutants and control mice (Figure 3).

Discussion

We show in this study that mice with *Per1/Per2* double mutations displayed an early onset of decrease in the female fertility. However, there was no obvious change with vascular growth associated with the ovarian follicles and in other tissues examined in the mutant mice. Interestingly, we found that there was a significant reduction of the ovarian follicle number in the *Per1/Per2* mutants from the middle-aged stage onwards compared with the littermate controls. The process of ovarian follicle development is tightly controlled by many factors. It is possible that *Per1/Per2* loss-of-function mutations may alter gene expression involved in the follicular development, leading to the depletion of the ovarian follicle reserve and the decline of reproductive capacity.

It was previously demonstrated that deletion of *Per1* or *Per2* affected female fertility at the age of 9–12 months old displaying abnormal oestrous cycle and reduced implantation success, but there was no obvious difference observed with young adult mutants (2–6 months old) [15]. In this study, we found that the doubly *Per1/Per2*

Table 2. Quantification of ovarian follicle number at different development stages of *Per1*$^{m/m}$*; Per2*$^{m/m}$ doubly mutant and control mice (3, 8, 26, 52 weeks old).

Ovarian follicle stages	Ovarian follicle number (3 weeks old)		n (*Per1*$^{m/m}$;*Per2*$^{m/m}$)	n (*Control*)	*P* value
	Per1$^{m/m}$;*Per2*$^{m/m}$	*Control*			
Ovarian follicle number (3 weeks old)					
Primordial	1356.00 ± 307.05	1642.00 ± 634.34	5	5	0.39068631
Primary	162.00 ± 23.61	165.00 ± 53.85	5	5	0.911982313
Secondary	343.00 ± 102.02	337.00 ± 45.36	5	5	0.90731292
Antral	55.00 ± 12.75	53.00 ± 54.15	5	5	0.937904244
Total	1916.00 ± 370.18	2197.00 ± 692.08	5	5	0.446499944
Ovarian follicle number (8 weeks old)					
Ovarian follicle stages	Ovarian follicle number (8 weeks old)		n (*Per1*$^{m/m}$;*Per2*$^{m/m}$)	n (*Control*)	*P* value
	Per1$^{m/m}$;*Per2*$^{m/m}$	*Control*			
Primordial	151.67 ± 80.04	222.00 ± 95.43	9	5	0.185634764
Primary	177.78 ± 57.29	177.00 ± 61.85	9	5	0.98228293
Secondary	211.11 ± 70.70	174.00 ± 86.16	9	5	0.422737236
Antral	91.11 ± 24.21	61.00 ± 25.38	9	5	0.057257555
Total	631.67 ± 172.92	634.00 ± 248.26	9	5	0.984694705
Ovarian follicle number (26 weeks old)					
Ovarian follicle stages	Ovarian follicle number (26 weeks old)		n (*Per1*$^{m/m}$;*Per2*$^{m/m}$)	n (*Control*)	*P* value
	Per1$^{m/m}$;*Per2*$^{m/m}$	*Control*			
Primordial	60.00 ± 43.09	95.91 ± 41.76	11	8	0.085424818
Primary	94.38 ± 51.79	148.18 ± 40.64	11	8	0.021065468
Secondary	72.50 ± 35.36	138.18 ± 24.73	11	8	0.000173887
Antral	41.88 ± 13.61	53.64 ± 32.41	11	8	0.350178113
Total	268.75 ± 103.71	435.91 ± 85.81	11	8	0.001301834
Ovarian follicle number (52-week-old)					
Ovarian follicle stages	Ovarian follicle number (52 weeks old)		n (*Per1*$^{m/m}$;*Per2*$^{m/m}$)	n (*Control*)	*P* value
	Per1$^{m/m}$;*Per2*$^{m/m}$	*Control*			
Primordial	27.14 ± 19.19	51.25 ± 35.87	14	12	0.039192918
Primary	25.00 ± 19.12	52.50 ± 12.88	14	12	0.000299226
Secondary	23.93 ± 11.12	41.67 ± 25.35	14	12	0.026081444
Antral	12.14 ± 7.26	22.50 ± 13.23	14	12	0.018619029
Total	88.21 ± 48.70	167.92 ± 59.29	14	12	0.00095254

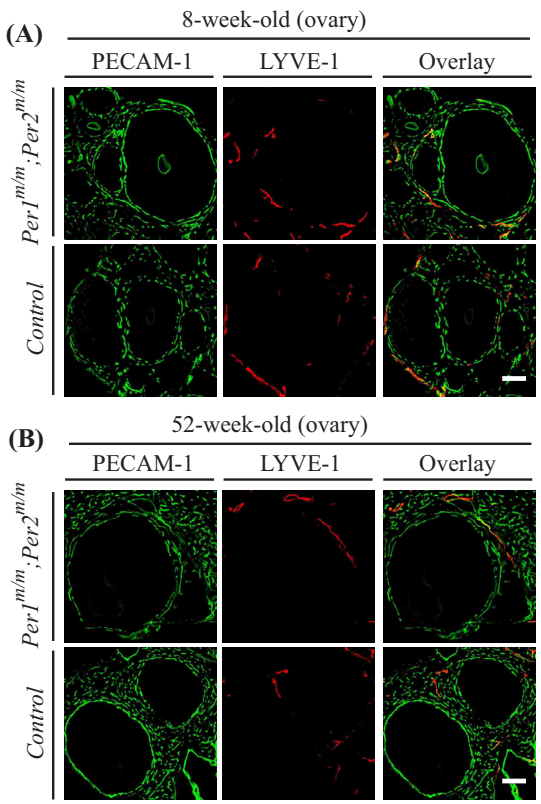

Figure 3. Analysis of vascular formation in ovaries of *Per1*$^{m/m}$*; Per2*$^{m/m}$ doubly mutant mice. (A, B) Immunostaining analysis of blood vascular and lymphatic vessels in ovaries of 8 weeks old (A) and 52 weeks old (B) *Per1*$^{m/m}$*; Per2*$^{m/m}$ mutant and control mice (PECAM-1, green; LYVE-1, red). Scale bar: 100 μm.

mutations caused an earlier onset of decrease in the female fertility than that of single mutation, suggesting a synergistic effect of PER1 and PER2 in reproduction. The phenotype was observed starting from 20 weeks old with significantly less pups delivered at the stage of 32 weeks old. Consistently, there was a significant decrease of ovarian follicles in the *Per1/Per2* double mutants compared with the control mice examined at 26 and 52 weeks old, while the total number of ovarian follicles was similar between the two groups at young ages (3 and 8 weeks old). This suggests that the abnormal decline of ovarian follicle reserve observed in the adult *Per1/Per2* mutants contributes to their reduced fertility, in addition to other causes as previously reported [15].

Pathogenesis underlying POI is still incompletely understood and may involve a wide spectrum of causes. Of the causative factors of genetic origin, more than 50 genes have been identified as POI candidates, which are involved in various processes such as oogenesis and folliculogenesis [1, 2]. Among the causative candidates, abnormal hormonal signaling including the follicle-stimulating hormone (FSH) receptor-mediated pathway may be one of the major contributors of POI [1]. It is known that the primary circadian pacemaker in the SCN provides a central control for the expression of core clock genes as well as clock-controlled genes, including the release of FSH and LH with a diurnal rhythm [14]. Furthermore, rhythmic expression of *Per1* and *Per2* was detected in the steroidogenic cells of preantral, antral, and preovulatory follicles as well as corpora lutea [10]. Accumulating evidences indicate that the circadian clock plays an important role in the amplitude and timing of ovarian steroid hormone synthesis, oocyte maturation, and ovulation [14]. Alteration of estrogen-mediated signaling could affect the follicular pool [26, 27]. Consistently, it has been found that disruption of circadian rhythm produces a negative effect on fertility in rodent models and women exposed to shiftwork schedules [14]. It is therefore likely that disruption of circadian rhythm or clock-regulated gene network by the *Per1/Per2* mutation may contribute to the occurrence of POI by affecting the reproductive endocrine system at possibly each level of the hypothalamic–pituitary–ovarian axis.

While clock genes were reported to regulate angiogenesis in zebrafish [22], we did not observe any obvious difference in vascular development in several tissues examined including retina, skin, trachea, and uterus from the *Per1/Per2* mutant and control mice. Consistently, the reduced female fertility caused by *Per1/Per2* double mutations is not due to the alteration of vascular components associated with ovarian follicle development. It is possible that the distinct vascular phenotype may result from the species difference between zebrafish and mouse in the regulation of vascular formation by circadian clock genes. However, due to the potential for off-target effects by the use of antisense morpholinos [28], it is necessary to validate the vascular phenotypes using knockout models targeting zebrafish *per2* or *bmal1*.

In summary, we found in this study that *Per1/Per2* double mutations caused a significant decrease of ovarian follicles in mutant mice from the middle-aged stage onwards. Although the detailed mechanism remains a topic for further investigation, findings of this study showed that the alteration of circadian rhythm and its underlying regulatory network could be an important factor contributing to the pathogenesis of POI. Future studies in this direction may yield more mechanistic insights into POI and provide potential therapeutic targets for the disease.

Supplemental Data

Supplementary data are available at *BIOLRE* online.

Supplemental Figure S1. Analysis of apoptosis in ovaries of *Per1*$^{m/m}$*; Per2*$^{m/m}$ doubly mutant and control mice. (A) Immunostaining analysis of apoptotic cells in ovaries (3 weeks old) of *Per1*$^{m/m}$*; Per2*$^{m/m}$ mutant and control mice (cleaved caspase 3, red; PECAM-1, green; LYVE-1, red; DAPI, blue). (B) Quntification of apoptotic cells (per grid, ×40 magnification). Scale bar: 50 μm in A.

Supplemental Figure S2. Analysis of vascular growth in retina and skin of *Per1*$^{m/m}$*; Per2*$^{m/m}$ doubly mutant and control neonatal mice (P5). (A, B) Immunostaining analysis of blood vascular and lymphatic vessels in retina (A) and skin (B) of *Per1*$^{m/m}$*; Per2*$^{m/m}$ mutant and control mice (P5, postnatal day 5; PECAM-1, green; LYVE-1, red). Quantification of retina vascularization area showed that there was no significant difference detected among *Per1/Per2* mutant and control mice (A; WT: 46.25 ± 2.93%, n = 6; *Per1*$^{+/m}$*; Per2*$^{+/m}$: 46.97 ± 5.16%, n = 6; *Per1*$^{m/m}$*; Per2*$^{m/m}$: 48.52 ± 5.39, n = 9). Scale bar: 100 μm in A and B.

Supplemental Figure S3. Analysis of vascular growth in adult tissues of *Per1*$^{m/m}$*; Per2*$^{m/m}$ doubly mutant and control mice. (A–C) Immunostaining analysis of blood vascular and lymphatic vessels in ear skin (A, 7 weeks old), trachea (B, 7 weeks old), and uterus (C, 8 and 52 weeks old) of *Per1*$^{m/m}$*; Per2*$^{m/m}$ mutant and control mice (PECAM-1, green; LYVE-1, red). Scale bar: 100 μm in A, B, and C.

Acknowledgment

We thank the staff in Animal facility of Soochow University for technical assistance.

Reference

1. Tucker EJ, Grover SR, Bachelot A, Touraine P, Sinclair AH. Premature ovarian insufficiency: new perspectives on genetic cause and phenotypic spectrum. *Endocr Rev* 2016; **37**:609–635.
2. Jiao X, Ke H, Qin Y, Chen ZJ. Molecular genetics of premature ovarian insufficiency. *Trends Endocrinol Metab* 2018; **29**:795–807.
3. de la Iglesia HO, Schwartz WJ. Minireview: timely ovulation: circadian regulation of the female hypothalamo-pituitary-gonadal axis. *Endocrinology* 2006; **147**:1148–1153.
4. Mohawk JA, Green CB, Takahashi JS. Central and peripheral circadian clocks in mammals. *Annu Rev Neurosci* 2012; **35**:445–462.
5. Albrecht U. Timing to perfection: the biology of central and peripheral circadian clocks. *Neuron* 2012; **74**:246–260.
6. Hastings MH, Reddy AB, Maywood ES. A clockwork web: circadian timing in brain and periphery, in health and disease. *Nat Rev Neurosci* 2003; **4**:649–661.
7. Zheng B, Albrecht U, Kaasik K, Sage M, Lu W, Vaishnav S, Li Q, Sun ZS, Eichele G, Bradley A, Lee CC. Nonredundant roles of the mPer1 and mPer2 genes in the mammalian circadian clock. *Cell* 2001; **105**:683–694.
8. Zheng B, Larkin DW, Albrecht U, Sun ZS, Sage M, Eichele G, Lee CC, Bradley A. The mPer2 gene encodes a functional component of the mammalian circadian clock. *Nature* 1999; **400**:169–173.
9. Xu Y, Toh KL, Jones CR, Shin JY, Fu YH, Ptacek LJ. Modeling of a human circadian mutation yields insights into clock regulation by PER2. *Cell* 2007; **128**:59–70.
10. Fahrenkrug J, Georg B, Hannibal J, Hindersson P, Gras S. Diurnal rhythmicity of the clock genes Per1 and Per2 in the rat ovary. *Endocrinology* 2006; **147**:3769–3776.
11. Karman BN, Tischkau SA. Circadian clock gene expression in the ovary: effects of luteinizing hormone. *Biol Reprod* 2006; **75**:624–632.
12. Chappell PE. Clocks and the black box: circadian influences on gonadotropin-releasing hormone secretion. *J Neuroendocrinol* 2005; **17**:119–130.
13. Sitzmann BD, Lemos DR, Ottinger MA, Urbanski HF. Effects of age on clock gene expression in the rhesus macaque pituitary gland. *Neurobiol Aging* 2010; **31**:696–705.
14. Sellix MT. Circadian clock function in the mammalian ovary. *J Biol Rhythms* 2015; **30**:7–19.
15. Pilorz V, Steinlechner S. Low reproductive success in Per1 and Per2 mutant mouse females due to accelerated ageing? *Reproduction* 2008; **135**:559–568.
16. Miller BH, Olson SL, Turek FW, Levine JE, Horton TH, Takahashi JS. Circadian clock mutation disrupts estrous cyclicity and maintenance of pregnancy. *Curr Biol* 2004; **14**:1367–1373.
17. Ratajczak CK, Boehle KL, Muglia LJ. Impaired steroidogenesis and implantation failure in Bmal1–/– mice. *Endocrinology* 2009; **150**:1879–1885.
18. Tsuji T, Kiyosu C, Akiyama K, Kunieda T. CNP/NPR2 signaling maintains oocyte meiotic arrest in early antral follicles and is suppressed by EGFR-mediated signaling in preovulatory follicles. *Mol Reprod Dev* 2012; **79**:795–802.
19. Liu Y, Johnson BP, Shen AL, Wallisser JA, Krentz KJ, Moran SM, Sullivan R, Glover E, Parlow AF, Drinkwater NR, Schuler LA, Bradfield CA. Loss of BMAL1 in ovarian steroidogenic cells results in implantation failure in female mice. *Proc Natl Acad Sci USA* 2014; **111**:14295–14300.
20. Mereness AL, Murphy ZC, Forrestel AC, Butler S, Ko C, Richards JS, Sellix MT. Conditional deletion of Bmal1 in ovarian theca cells disrupts ovulation in female mice. *Endocrinology* 2016; **157**:913–927.
21. Viswambharan H, Carvas JM, Antic V, Marecic A, Jud C, Zaugg CE, Ming XF, Montani JP, Albrecht U, Yang Z. Mutation of the circadian clock gene Per2 alters vascular endothelial function. *Circulation* 2007; **115**:2188–2195.
22. Jensen LD, Cao Z, Nakamura M, Yang Y, Brautigam L, Andersson P, Zhang Y, Wahlberg E, Lanne T, Hosaka K, Cao Y. Opposing effects of circadian clock genes Bmal1 and Period2 in regulation of VEGF-dependent angiogenesis in developing zebrafish. *Cell Rep* 2012; **2**:231–241.
23. Ferrara N. Vascular endothelial growth factor: basic science and clinical progress. *Endocr Rev* 2004; **25**:581–611.
24. Chu M, Li T, Shen B, Cao X, Zhong H, Zhang L, Zhou F, Ma W, Jiang H, Xie P, Liu Z, Dong N et al. Angiopoietin receptor Tie2 is required for vein specification and maintenance via regulating COUP-TFII. *eLife* 2016; **5**:e21032.
25. Bae K, Jin X, Maywood ES, Hastings MH, Reppert SM, Weaver DR. Differential functions of mPer1, mPer2, and mPer3 in the SCN circadian clock. *Neuron* 2001; **30**:525–536.
26. Zangen D, Kaufman Y, Zeligson S, Perlberg S, Fridman H, Kanaan M, Abdulhadi-Atwan M, Abu Libdeh A, Gussow A, Kisslov I, Carmel L, Renbaum P et al. XX ovarian dysgenesis is caused by a PSMC3IP/HOP2 mutation that abolishes coactivation of estrogen-driven transcription. *Am J Hum Genet* 2011; **89**:572–579.
27. Chen Y, Breen K, Pepling ME. Estrogen can signal through multiple pathways to regulate oocyte cyst breakdown and primordial follicle assembly in the neonatal mouse ovary. *J Endocrinol* 2009; **202**:407–417.
28. Kok FO, Shin M, Ni CW, Gupta A, Grosse AS, van Impel A, Kirchmaier BC, Peterson-Maduro J, Kourkoulis G, Male I, DeSantis DF, Sheppard-Tindell S et al. Reverse genetic screening reveals poor correlation between morpholino-induced and mutant phenotypes in zebrafish. *Dev Cell* 2015; **32**:97–108.